# High Fidelity VSF Measurements and Inversion for RaDyO (Hi Fi RaDyO)

Michael Twardowski
Department of Research
WET Labs, Inc.
70 Dean Knauss Dr
Narragansett, RI 02882
phone: (401)783-1787 fax: (401)783-0309 email: mtwardo@wetlabs2.com

Ron Zaneveld
Department of Research
WET Labs, Inc.
620 Applegate St
Philomath, OR 97370
phone: (541)929-5650 fax: (541)929-5277 email: ron@wetlabs.com

Contract Number: N0001406C0027
http://www.wetlabs.com

## LONG TERM GOALS

Time and space dependent radiance distributions at the sea surface are a function of the shape of the incident distribution on the surface, modification by the sea surface itself from topography and transmission characteristics, and alteration by the Inherent Optical Properties (IOPs) of the surface ocean. Our long term goal is understanding this last controlling factor. With a knowledge of the IOPs, radiance fields can be directly computed from the incident field using the equation of radiative transfer, now embedded in commercially available code (e.g., Hydrolight).

With the state of current technology and methodologies, the primary obstacles in understanding subsurface IOPs and their high-frequency dynamics are a lack of 1) volume scattering instrumentation, 2) comprehensive inversion models linking the IOPs with the ambient particle fields including bubbles (models which in many cases will require input dependent on 1), and 3) suitably stable, non-intrusive platforms to sample the subsurface ocean. The first two challenges are addressed in this project.

## OBJECTIVES

There are two broad objectives for this project:

1) To develop an in-situ volume scattering function device measuring volume scattering from 10° to 170° at 10° intervals and sampling rates of 1 $s^{-1}$ or better to sample the VSF in near-surface waters; and

# Report Documentation Page

*Form Approved*
*OMB No. 0704-0188*



| 1. REPORT DATE | 2. REPORT TYPE | 3. DATES COVERED |
|---|---|---|
| **2010** | | **00-00-2010 to 00-00-2010** |

| 4. TITLE AND SUBTITLE | |
|---|---|
| **High Fidelity VSF Measurements and Inversion for RaDyO (Hi Fi RaDyO)** | 5a. CONTRACT NUMBER |
| | 5b. GRANT NUMBER |
| | 5c. PROGRAM ELEMENT NUMBER |
| 6. AUTHOR(S) | 5d. PROJECT NUMBER |
| | 5e. TASK NUMBER |
| | 5f. WORK UNIT NUMBER |
| 7. PERFORMING ORGANIZATION NAME(S) AND ADDRESS(ES)<br>**WET Labs, Inc.,Department of Research,70 Dean Knauss Dr,Narragansett,RI,02882** | 8. PERFORMING ORGANIZATION REPORT NUMBER |
| 9. SPONSORING/MONITORING AGENCY NAME(S) AND ADDRESS(ES) | 10. SPONSOR/MONITOR'S ACRONYM(S) |
| | 11. SPONSOR/MONITOR'S REPORT NUMBER(S) |

12. DISTRIBUTION/AVAILABILITY STATEMENT

**Approved for public release; distribution unlimited**

13. SUPPLEMENTARY NOTES

14. ABSTRACT

15. SUBJECT TERMS

| 16. SECURITY CLASSIFICATION OF: | | | 17. LIMITATION OF ABSTRACT | 18. NUMBER OF PAGES | 19a. NAME OF RESPONSIBLE PERSON |
|---|---|---|---|---|---|
| a. REPORT | b. ABSTRACT | c. THIS PAGE | | | |
| **unclassified** | **unclassified** | **unclassified** | **Same as Report (SAR)** | **22** | |

2) To develop and refine IOP inversion models to resolve particle field characteristics on small spatial (cm's) and temporal (<1 s) scales in near-surface waters.

## APPROACH

Our design for the VSF device is illustrated in **Figure 1**. The device is called MASCOT (Multi-Angle SCattering Optical Tool). The source beam is a 30 mW 658 nm laser diode expanded with a Gallilean 2X beam expander to an approximately 3 mm X 8 mm elliptical shape. A wedge depolarizer is used to provide the unpolarized light needed for VSF determinations. Seventeen independent silicon diode detectors spaced in a semicircle 10 cm around the sample volume measure volume scattering from 10° to 170° at 10° intervals. The total pathlength for all scattering measurements is 20 cm. Independent detectors allow resolution of the VSF without any moving parts and time-consuming scanning. Additionally, each detector can be optimized for its specific dynamic range. Detector field-of-views (FOVs) range from 0.8° to 5° for the different detectors, with the narrowest FOVs associated with the detectors measuring scattering in the forward direction. Using proprietary electronics, a 20 Hz sampling rate for all channels has been achieved while maintaining a worst case signal:noise of 300:1. Relatively fast sampling rates are important in resolving VSFs in the highly dynamic ocean subsurface.

Polarized VSFs have now been successfully collected with the addition of filter mount placed in front of the source beam. A linear polarizer is used to obtain scattering from a vertically and horizontally polarized source (in terms of the Mueller scattering matrix elements, (S11+S12)/2 and (S11-S12)/2 are measured, so that S11 and S12 may be derived). Adding polarized scattering increases the amount of information on particle characteristics we are collecting, and is expected to improve our ability to discriminate different particle types (both the number of subpopulations and the accuracy of individual determinations). The degree of linear polarization (S12/S11) is most dependent on the degree of sphericity, particle size, and refractive index.

For VSF inversion modeling, we are extending the capabilities of existing models (Twardowski et al. 2001; Twardowski and Zaneveld, 2004; Zhang et al. 2005) by incorporating input from new VSF measurements and by adding bubble particle populations (clean and coated) in the models. Candidate phase functions for particle subpopulations are fit to measured VSFs using a least-squares minimization matrix inversion procedure. These phase functions can be obtained theoretically using Mie theory, DDA, or IGOM techniques, or experimentally in controlled laboratory conditions. George Kattawar's group has recently provided married DDA-IGOM phase function determinations for asymmetric polyhedrons we are now using in the inversions.

The MASCOT has now been extensively deployed concurrently with the commercially available near-forward VSF device LISST (Sequoia Inc.) in order to capture the VSF with good resolution from ~0.1 degrees to 170 degrees. Our deployment package also contains CTD, AC9 (or ACS), and various ECO scattering sensors, all integrated in a vertical profiling system (**Figure 2)**.

Deployments for RaDyO have taken place in collaboration with other RaDyO investigators off Scripps Pier in January 2008, in Santa Barbara Channel in September 2008, and off Hawaii in September 2009. For these RaDyO deployments, we have also intermittently integrated two additional sensors: 1) a high sampling rate fish-eye lens radiometer currently being developed by Marlon Lewis and Scott McLean of Satlantic, and 2) a bubble acoustic resonator developed by Svein Vagle, David Farmer, and Helen

Czerski. For the Scripps Pier experiment, a mobile deployment platform was configured so that measurements could be made along the length of the pier, with the expectation that higher concentrations of bubbles would be observed nearing the surfzone. For subsequent field work in SBC and Hawaii, we are deploying our sensor package off the R/V Kilo Moana.

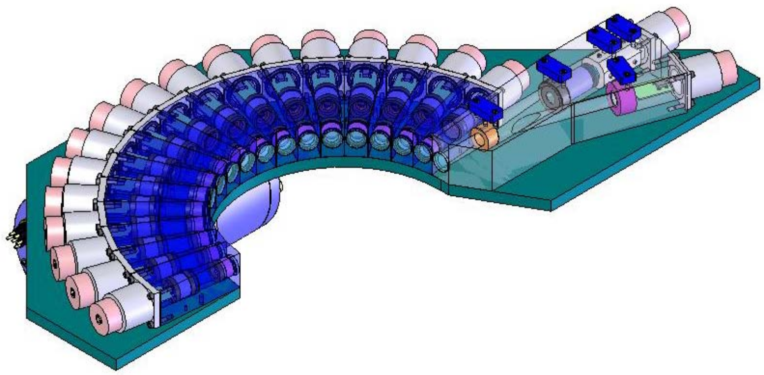

***Figure 1. Oblique view illustration of the MASCOT. The VSF is resolved from 10 to 170 degrees in 10 degree intervals. Detectors are wedge shaped and arranged in a semi-circle on an aluminum frame to minimize reflections and perturbation of the water sample in the remote volume (center of semi-circle). The source assembly includes a 30 mW 658 nm laser diode, reference detector, beam expander, and wedge depolarizer. Wiring from all the detector modules and the source module feeds to a data handling unit.***

**WORK COMPLETED**

- An IOP package including the MASCOT and LISST was deployed off Scripps Pier, in the Santa Barbara Channel, and off Hawaii during collaborative RADYO exercises.
- The MASCOT was adapted to additionally measure linear polarized scattering elements to derive degree of linear polarization (DOLP) as a function of angle.
- An acoustic bubble resonator (Vagle and Farmer) and fish-eye lens camera (Lewis) were successfully integrated on the MASCOT IOP package and deployed for all exercises.
- The MASCOT IOP package was tested off the New York Bight in May and July 2009 in association with other funded work.
- A revised calibration protocol was developed and implemented, using clean techniques and accurately accounting for pure water absorption along the optical path.
- A revised calibration and correction protocol was developed for the LISST to account for optical geometry, ambient light contamination, turbulent scattering, and vignetting.
- A second MASCOT prototype with a larger dynamic range suitable for high turbidity environments (such as the surf zone) was tested in the lab and deployed in the NY Bight and the surf zone at Duck, NC.

- Inversion of MASCOT VSFs collected off Scripps Pier, SBC, and Hawaii into component VSFs associated with subpopulations of the bulk particle field including bubbles has been refined using a least-squares minimization matrix inversion model, including derivation of particle concentration and size distribution for each subpopulation. The model has been adapted to also invert for nonspherical asymmetric polyhedron particles more analogous to natural suspended mineral populations.
- Based on results from this project, 4 papers have been published by our group, 1 additional paper has been submitted, 2 additional papers are close to submission, and 2 additional papers are in preparation for the RaDyO JGR Special Issue.

**RESULTS**

**Fig. 2** shows the MASCOT device in a custom cage with additional optical sensors ready for deployment. Orientation in the horizontal plane minimizes any shear perturbation of the sampled water parcel during upcasts.

We have implemented the VSF inversions now with phase functions computed for nonspherical particles (asymmetric polyhedrons). These have been assimilated into our phase function library along with Mie theory derived phase functions for coated bubbles. Phase functions for asymmetric polyhedron monodispersions are shown in **Fig. 3**.

Inversion results from the Scripp's Pier surf zone using combinations of asymmetric polyhedron subpopulations (mineral-mimicking), coated spherical particles (bubbles) and Very Small Particles (VSPs) are shown in **Fig. 4.** The VSPs are quasi-Rayleigh scatterers with sizes near the wavelength of the source beam; for these particles, composition information is difficult to glean from scattering measurements alone. Inversion results are substantially more stable using the asymmetric polyhedron phase functions as opposed to previous phase functions where nonspherical particles were approximated with spheres. Particles dominated by sediments were present over the first hour of the time series, with bubbles becoming much more important as the surf zone approached our sampling area with the ebbing tide. **Fig. 5** shows the inverted subpopulation size distributions during the time period of localized wave breaking. This is the first time the theoretically expected mid-angle enhancement in scattering due bubbles has been observed in-situ. The 20 Hz sampling rate for all VSF channels allows sufficient resolution of the bubble plumes as they rapidly evolve in time and space. A very low background scattering condition (particle attenuation less than 0.3 $m^{-1}$ at 532 nm) enhanced our dynamic range in resolving intense scattering associated with episodic bubble and sediment plume generation.

Inversion results are encouraging and are consistent with anecdotal evidence (what we saw) with respect to patches of sediment and/or bubbles. **Fig. 6** shows the inversion results for the 2 primary sediment subpopulations, and **Fig. 7** shows results for the primary large bubble subpopulation. **Fig. 8** evaluates the use of $\beta(70)/\beta(120)$ as a proxy for large bubble subpopulation abundances. The positive correlation is encouraging, although more work is required to see if using specific bins in the larger size classes may improve the fit. **Fig. 9** shows acoustics data collected with the Svein/Farmer bubble resonator concurrently with the large bubble subpopulation from the inversion for the last 40 minutes of the **Fig. 6** time series. Very good agreement between patterns in optical scattering from bubbles (positive displacements of the $\beta(70)/\beta(120)$ relationship relative to the background) and acoustic attenuation at multiple frequencies was observed. **Fig. 10** shows the size distributions from the inversion results for one of the measured VSFs, with an aggregate distribution consistent with the familiar Junge-type distribution in the optically relevant size range (~0.1 to ~40 μm). Stable model solutions (only possible to assess with a very large number of VSFs) consistent with anecdotal observations of particle composition, coupled with validation based on acoustic measurements of bubble distributions and fractional and aggregate size distributions agreeing with theory and observations, provides strong evidence that our inversion results are environmentally meaningful.

We also able to leverage other ongoing work to deploy the MASCOT device along with the Farmer/Vagle/Czerski acoustic resonator in East Sound, WA in May 2010. This exercise helped evaluate the importance of surfactants in stabilizing bubble populations through coating of the bubbles. For the experiment, a collaborating boat passed off our bow at full throttle creating a linear propeller wash. Our boat then towed the MASCOT and resonator back and forth through the propeller wash along with a holographic camera from Joe Katz's group (JHU). Jim Churnside also participated in the experiment, flying lidar missions over the propeller wash. Substantial, repeatable signatures from bubbles were observed in the wash by the optical and acoustical techniques, with persistence for over 1 hour (**Fig. 11**). Similar measurements from the day before in waters with low surfactants revealed that propeller wash bubbles vanished after 10-15 minutes. Surfactants are thus very important in stabilizing near-surface bubble populations.

Preliminary inversion results from Hawaii for a time series where the acoustic bubble resonator was also deployed with the MASCOT are shown in **Fig.** 12. Interestingly, there is no evidence of a persistent small bubble population in this data set, as was observed in the inversion results from Scripp's Pier. During bubble injections and subsequent seconds of bubble plume evolution, the peaks in bubble size distributions were typically observed between 1-2 μm.

General observations from our VSF inversions and validation efforts can be summarized as:

- Patterns in bubble and mineral contributions indicate consistently stable solutions when nonspherical particles are considered (high number of VSFs essential to assess this)
- Patterns agree qualitatively with anecdotal observations
- Concurrent acoustic measurements corroborate large bubble inversion results
- PSDs from inversion results follow commonly observed Junge-type distribution reasonably well
- When modeling all particles as spheres, inversion is less stable, but most mineral and bubble subpopulation trends are accounted for

## IMPACT/APPLICATIONS

Progress and results represent important steps toward the development and vetting of a multi-angle, in-water VSF device. Knowledge of the Inherent Optical Properties including the VSF can be used to predict and optimize the performance of a host of Naval operations that rely on divers, cameras, laser imaging systems, and active and passive remote sensing systems. These include mine countermeasures, harbor security operations, debris field mapping, anti-submarine warfare, and search and salvage operations.

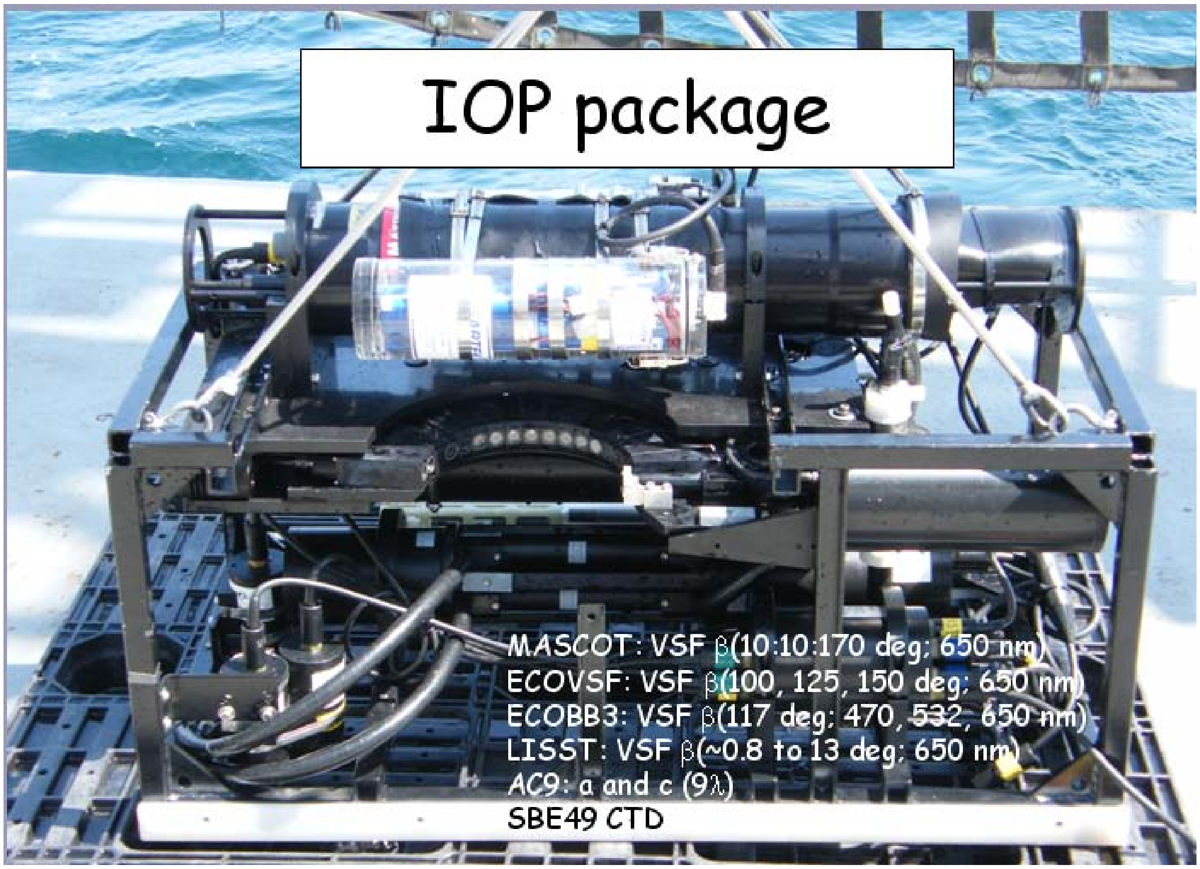


***Figure 2. MASCOT VSF device mounted with other optical sensors in a custom cage designed to sample the subsurface domain.***

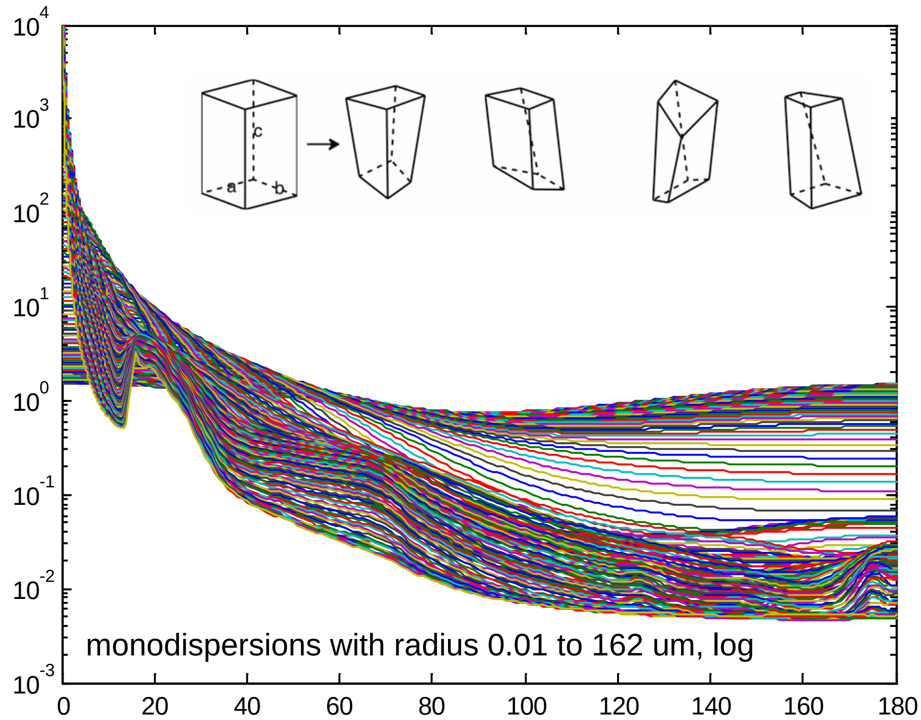


***Figure 3. Phase functions of asymmetric polyhedrons computed from a combination of the Discrete Dipole Approximation (DDA) and Improved Geometric Optics Model (IGOM) to span a wide range of particle sizes. Calculations were carried out in George Kattawar's lab in collaboration with Yu You and Li Bi. Asymmetric polyhedrons were generated by slightly adjusting the axes of a symmetric rectangular polyhedron to mimic the crystalline structure of mineral quartz.***

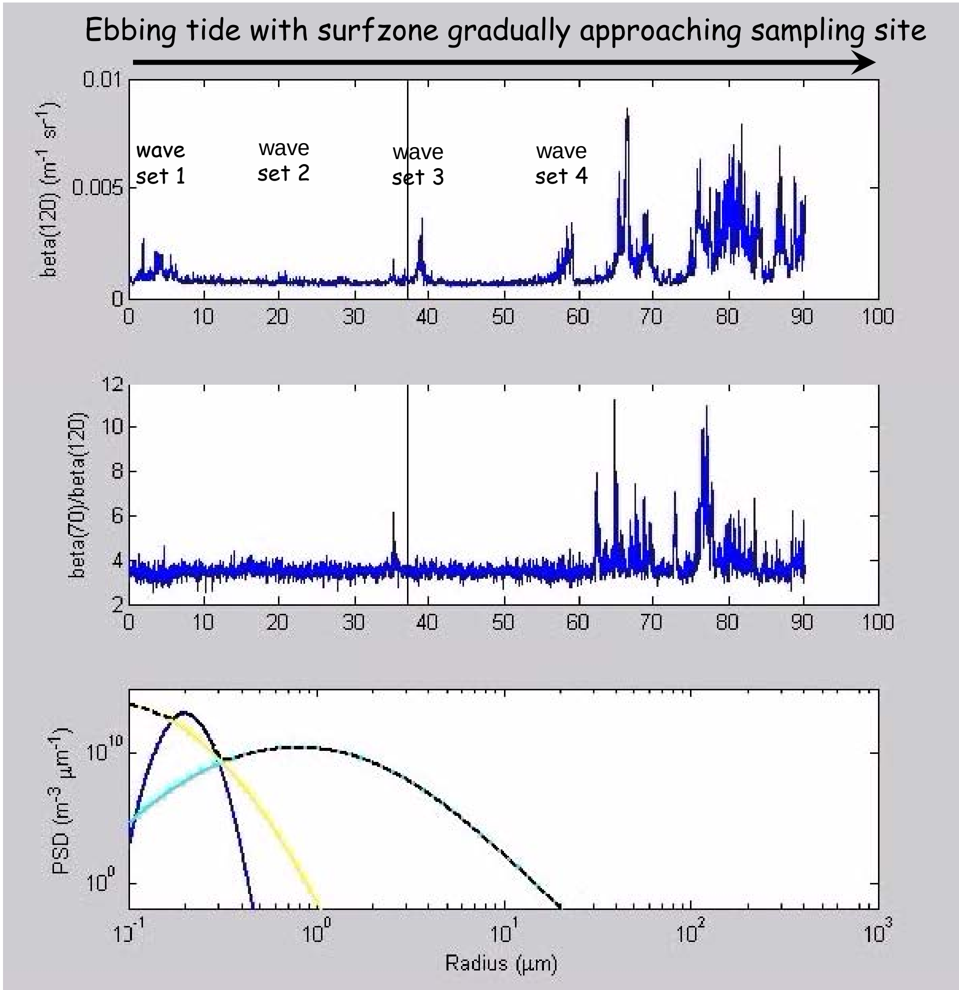


***Figure 4. Time series from VSF measurements off Scripp's Pier. Over time, the surf zone moved from a shoreward location to the vicinity of our sensing package with an ebbing tide. The VSF resolved at 120 degrees is plotted in the upper panel. In the first hour, 4 scattering events, marked as "wave sets" in the panel, were detected. Each involved a remnant sediment plume from shoreward surf zone resuspension that became entrained in a rip current running along the pier. Approximately 18 min separation between the plumes corresponded with primary wave sets hitting the surf zone. After the first hour, enhanced scattering is due to localized resuspension and bubble entrainment from breaking waves. The ratio of scattering at 70 deg to scattering at 120 deg is shown in the middle panel. Bubble particles exhibit enhanced scattering between 60 and 80 deg, so this ratio is a sensitive indicator of bubbles. Within the first hour, bubbles are only detected by this proxy ratio in a random local breaking event at 36 min. Afterward, substantial peaking of this ratio coincides with localized breaking and bubble injection. The bottom panel shows background particle population results from our VSF inversion for aggregate bubble populations (blue), aggregate mineral subpopulations (cyan) and "Very Small Particles" that cannot be distinguished in terms of composition. Mineral particles are observed to dominate the background population, with some evidence for a persistent small bubble population centered at about 0.2 µm.***

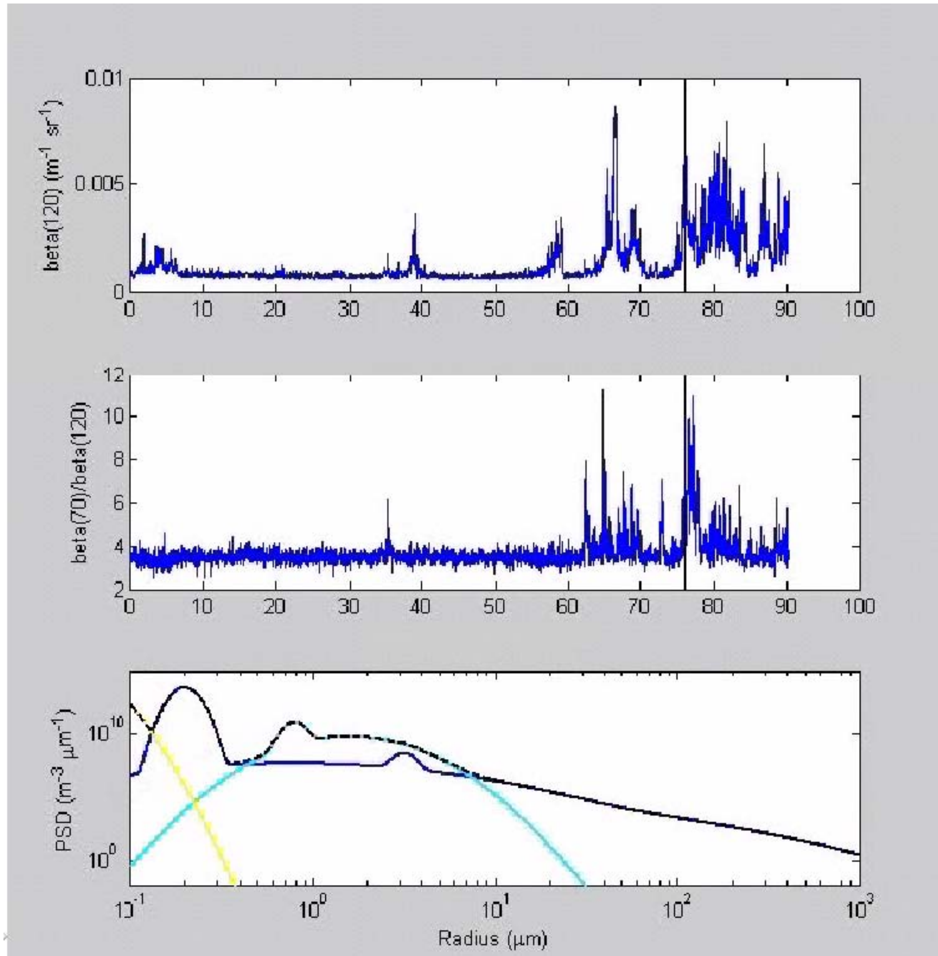


***Figure 5. Same as Fig. 4 except bottom panel shows inverted size distributions within a scattering peak dominated by bubbles from local injection. The distribution for minerals exhibits a broadening into larger size classes. The primary difference in these populations relative to the background, however, is a very substantial bubble population that dominates the larger particle sizes (> 20 µm).***

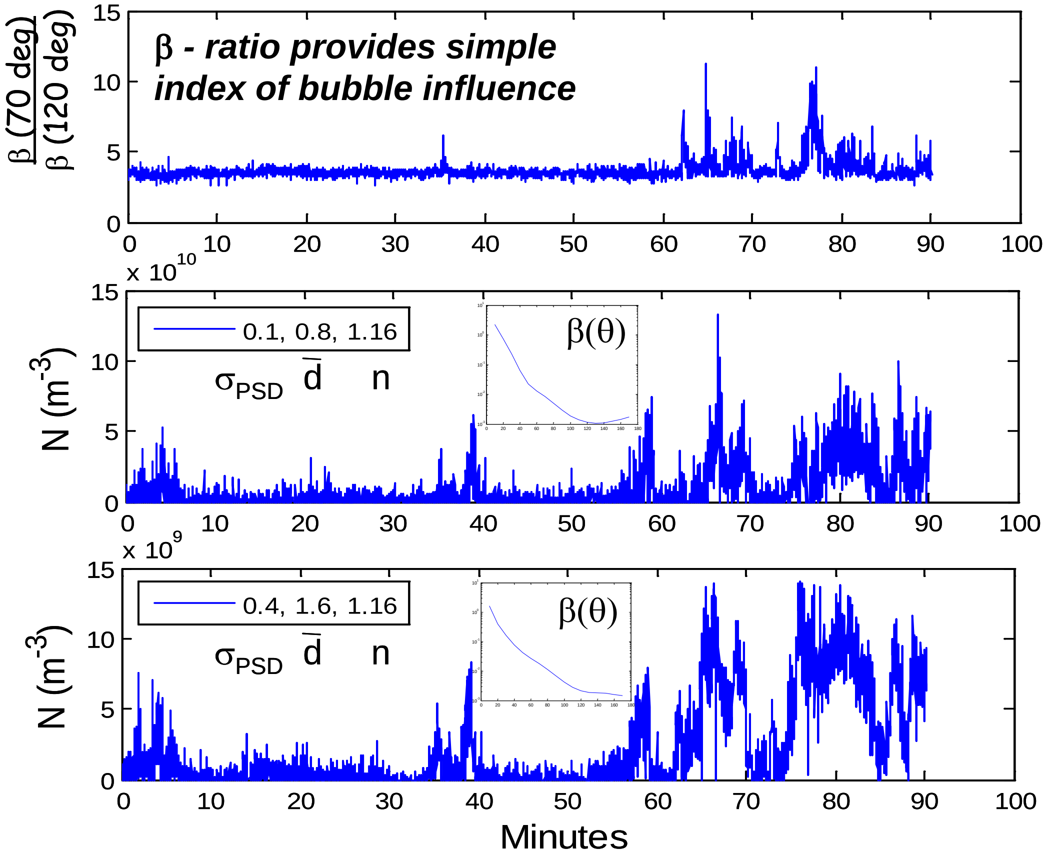


***Figure 6.** 3 panel plot showing the ratio of VSF at 70 deg to VSF at 120 deg, and the abundances for the two dominant sediment subpopulations over time. The bottom panel is the larger distribution. Substantial peaks are observed during the 4 sets within the first hour due to sediment plumes entrained in a rip current. Afterward, substantial abundances are observed in localized resuspension from wave breaking.*

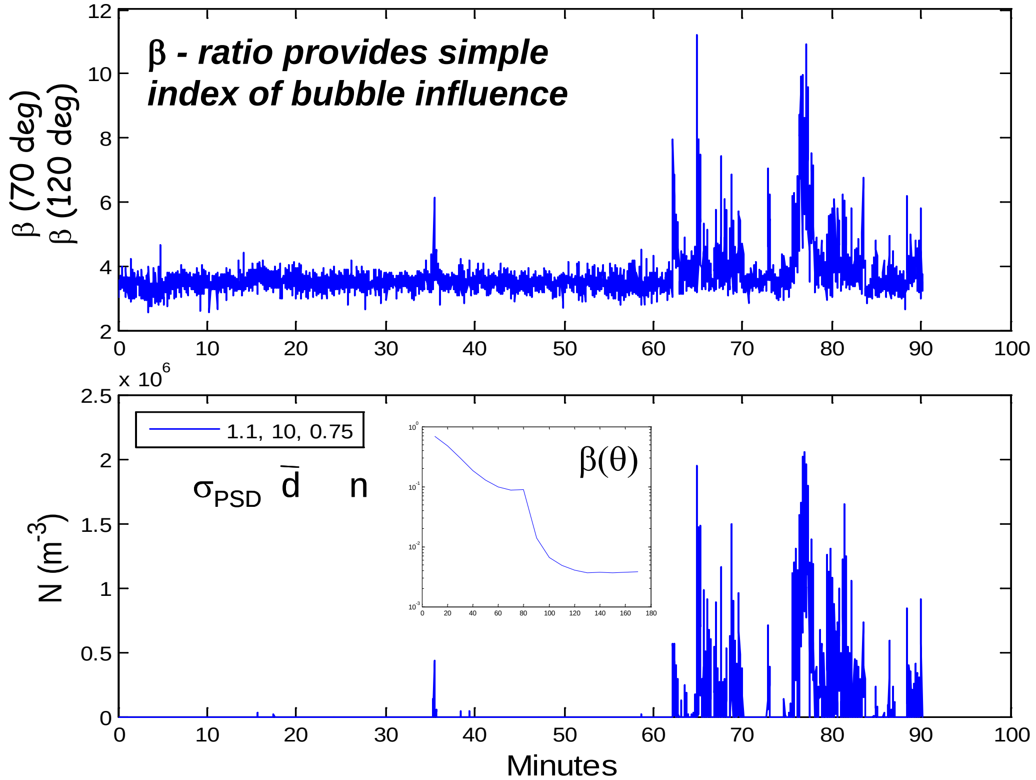


***Figure 7.  Plot showing the ratio of VSF at 70 deg to VSF at 120 deg (upper plot) and the dominant large bubble subpopulation (lower plot).  In the first hour, larges bubbles are only observed during a random local breaking event at 36 min. Substantial abundances of large bubbles are observed afterward in associated with localized wave breaking and bubble injection.***

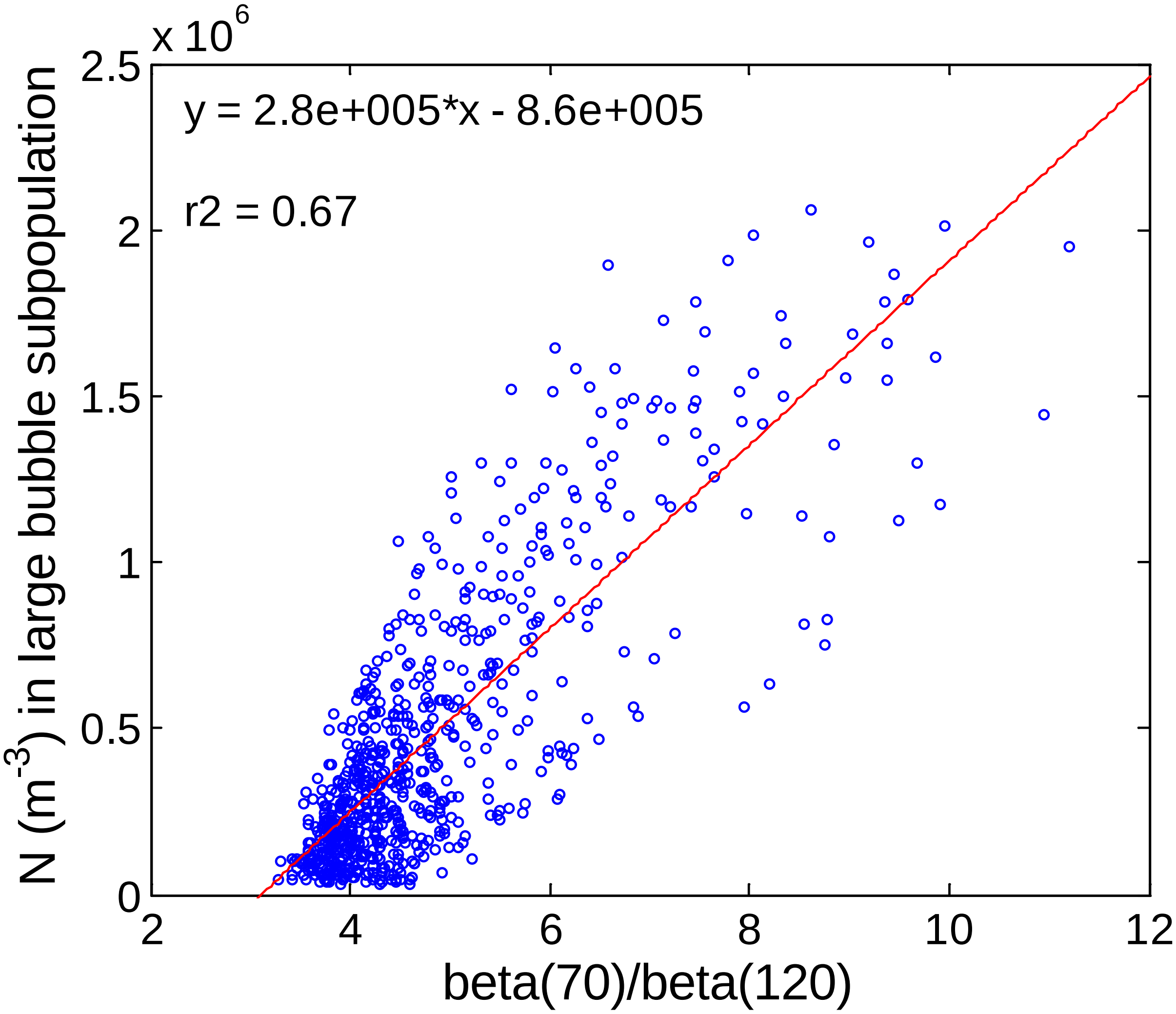


***Figure 8.** Large bubble subpopulation abundances from the VSF inversion plotted against the simple ratio of the VSF at 70 deg to VSF at 120 deg. A linear correlation is observed with an $r^2$ of 0.67, indicating that the ratio may be used as a simple proxy to approximate large bubble distributions over time.*

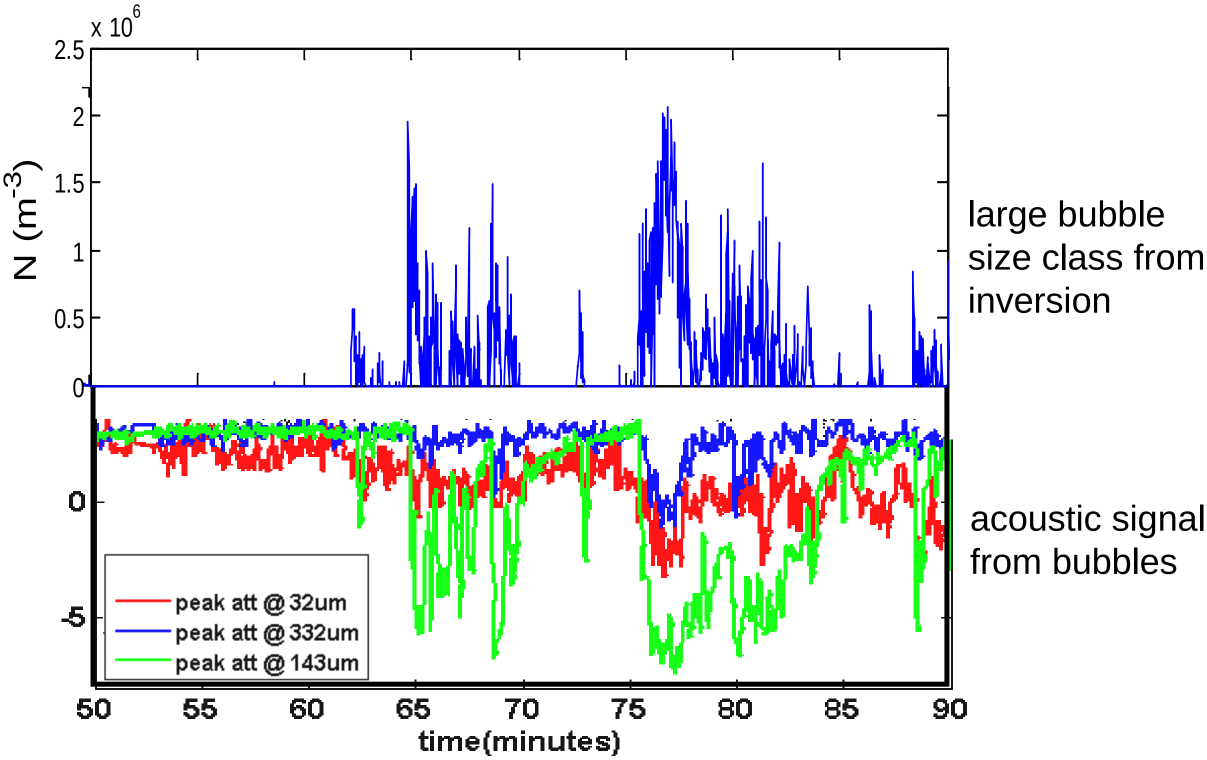


***Figure 9. Inversion results from the large bubble subpopulation (upper panel) plotted with relative acoustic attenuation from a bubble resonator (lower panel). Patterns were very consistent, more consistent than observed when comparing the acoustic attenuation with positive responses in β(70)/β(120) from the MASCOT. The time series shown here is a subset of the data shown in Figs. 4-7, including only wave sets 4 and 5. Note that the turbidity maximum observed around 58-60 minutes in Fig. 6 is not associated with any response from the acoustics or the inverted large bubble subpopulation. This is consistent with the previous interpretation that this turbidity plume is dominated by sediments. A particularly close agreement was observed between the inversion results and acoustic attenuation at the frequency specific for 143 um diameter bubbles. Note that even though the two sensors were on the same instrument package, sample volumes were separated by about 60 to 70 cm.***

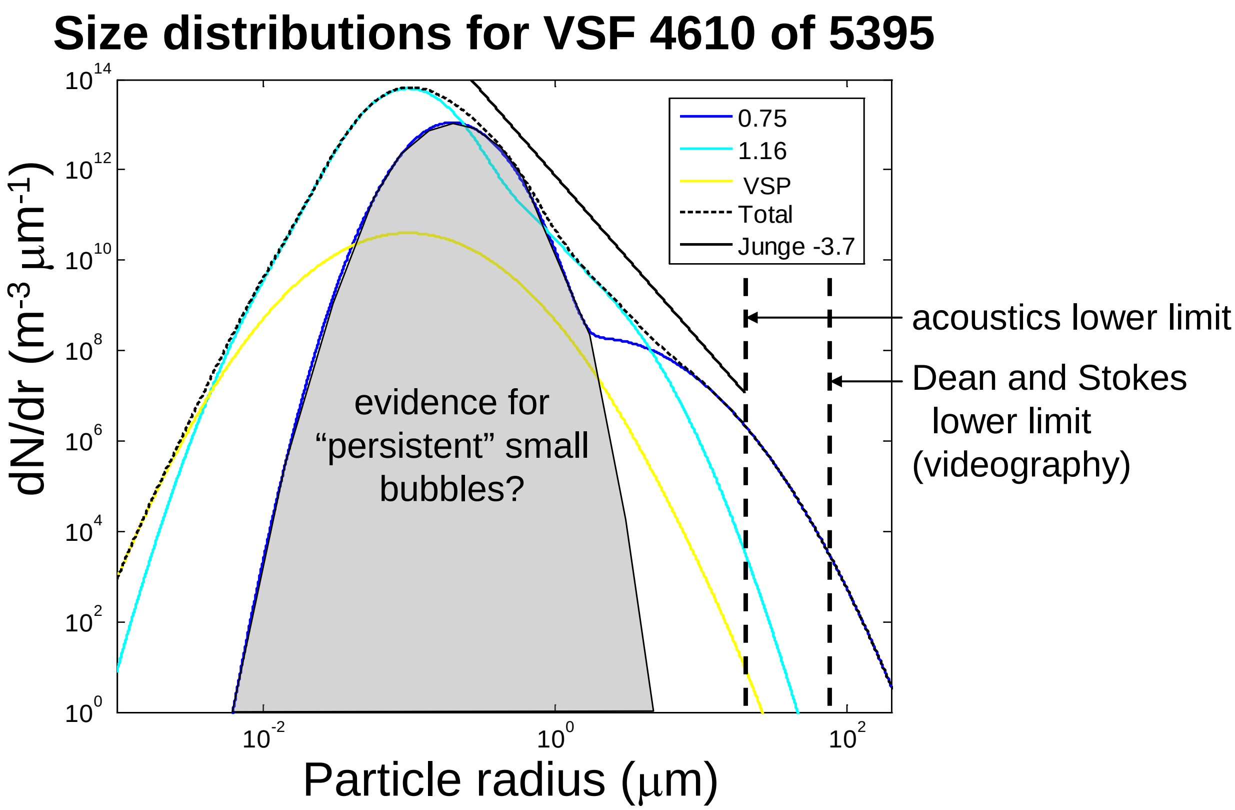


***Figure 10. Size distributions of dominant subpopulations with relative refractive indices of 0.75 (bubbles) and 1.16 (quartz-like minerals), and Very Small Particles (VSPs). The aggregate size distribution (in black) is modeled well with a hyperbolic differential Junge-type model with slope 3.7 in the range that can be resolved by sizing devices such as a Coulter Counter. Many previous studies looking at oceanic size distributions have observed that the Junge distribution is often a reasonable model, which serves as an element of validation for our inversion results.***

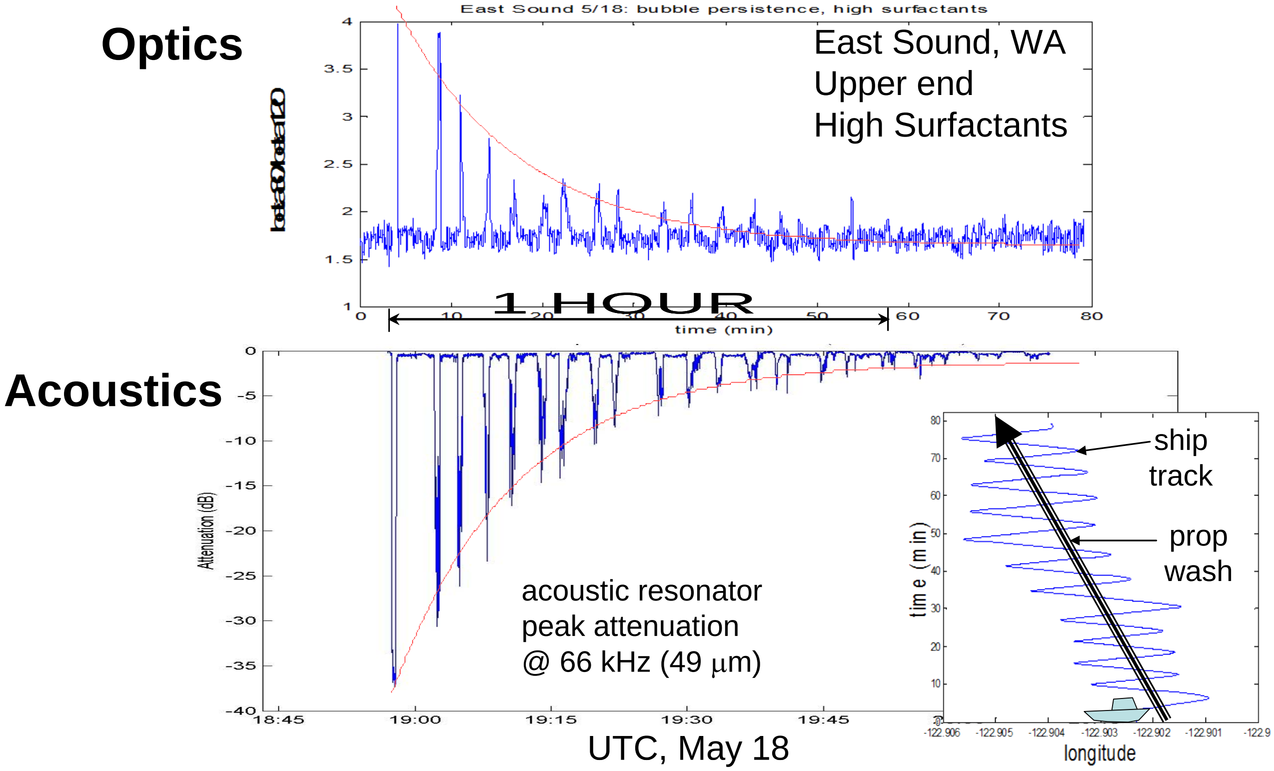


***Figure 11. Optical and acoustical evidence of bubble persistence behind a boat's propeller wash for over an hour in waters from East Sound, WA that exhibited high surfactant content. Previous data collected in waters with low surfactant showed bubble populations rapidly vanishing after 10-15 min. Data show the importance of surfactant coatings in stabilizing near-surface bubble populations.***

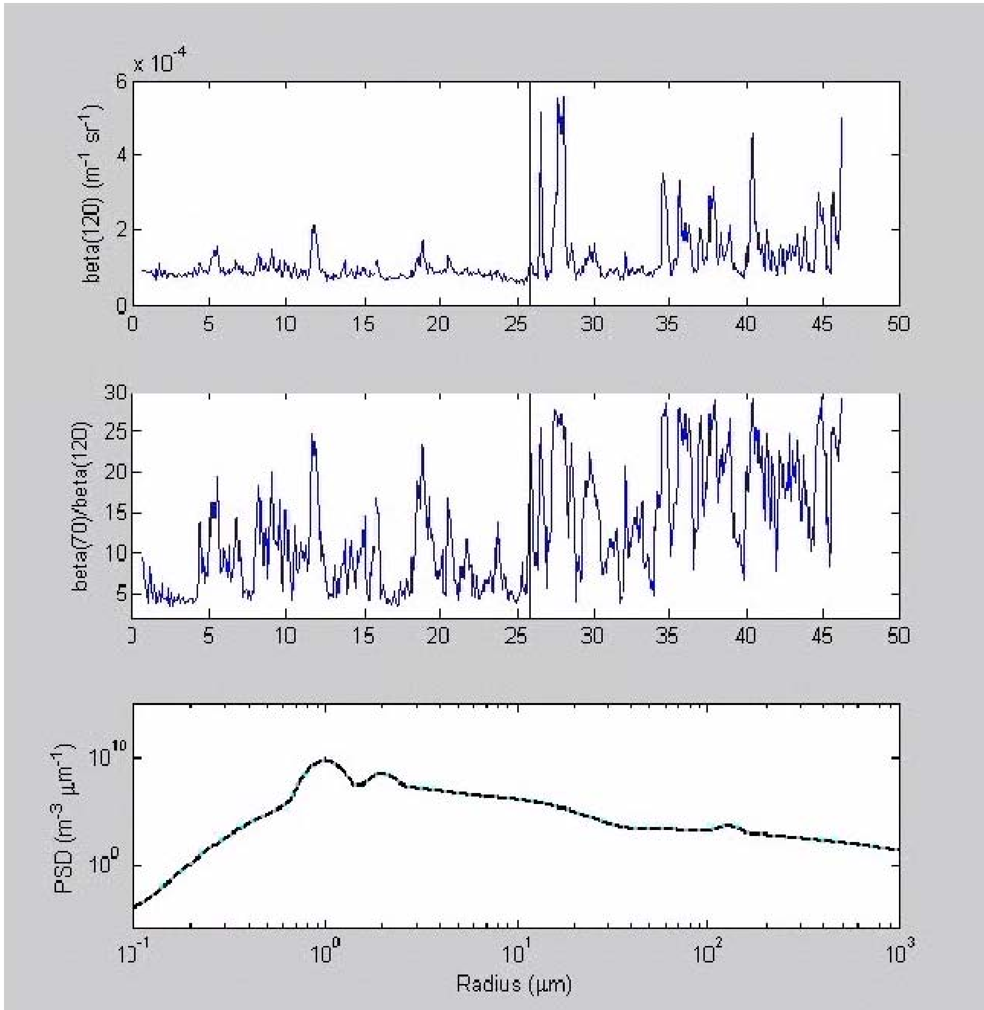


***Figure 12. Time series of scattering at 120 deg (upper panel), ratio of scattering at 70 deg to scattering at 120 deg (middle panel), and PSD inversion results for minute 26 (lower panel) for Hawaii data collected 09/2009. Phase function library for the inversion only included a background phase function and phase functions for bubble subpopulations computed from Mie theory. Interestingly, there is no evidence of a persistent small bubble population in this data set, as was observed in the inversion results from Scripp's Pier. During bubble injections and subsequent seconds of bubble plume evolution, the peaks in bubble size distributions were typically observed between 1-2 µm.***

## TRANSITIONS

We expect that our efforts in developing an in-water VSF device and associated inversion techniques to better understand particle dynamics in natural waters will lead to transition as operational tools for the fleet and the oceanographic research community in the future.

**RELATED PROJECTS**

This effort is related to several ongoing efforts by the PI to develop optical sensors and associated biogeochemical inversion techniques to improve our understanding of the oceanic environment. Current ongoing related projects include:

- investigating the dynamics of scattering by subsurface bubble populations and other particles in the S. Ocean (NASA, Twardowski; project lead PI H. Dierssen);
- investigating the underlying controls of biological camouflage responses in dynamic underwater optical environments (MURI collaboration, Twardowski; URI PIs J. Sullivan and B. Seibel; project lead PI M. Cummings);
- developing improved remote sensing water quality algorithms for coastal waters (NASA, Twardowski; project lead PI Z-P. Lee);
- developing compact, low power sensing tools for ocean observing platforms (ONR SBIR, Twardowski);
- developing a microscopic holographic camera for optically relevant particles (NOPP, project lead PI J. Sullivan);
- developing optical prediction models for the surfzone (CEROS, Twardowski; project lead PI G. Chang); and
- developing a surfzone drifter measuring optical attenuation and scattering (ONR SBIR, Twardowski).

**PUBLICATIONS**

**Twardowski**, M.S., J.M. Sullivan, P.L. Donaghay, and J.R.V. Zaneveld. 1999. Microscale quantification of the absorption by dissolved and particulate material in coastal waters with an ac-9. *J. Atmos. Ocean. Technol.* **16(12**):691-707. [refereed]

Boss, E., and M.S. **Twardowski**. 2000. On the relationship of the particulate beam attenuation spectrum and size distribution of oceanic particles. *Proceedings from Ocean Optics XV*, October 16-20, Monaco.

Coleman, J.E., R.A. Reynolds, M.C. Talbot, M.S. **Twardowski**, M.J. Perry. 2000. Utilization of solar-induced chlorophyll a fluorescence as an indicator of phytoplankton biomass in coastal waters. *Proceedings from Ocean Optics XV*, October 16-20, Monaco.

Eisner, L., M.S. **Twardowski**, and T.J. Cowles. 2000. In situ spectral absorption (ac-9) measurements as an index of photoprotective/photosynthetic carotenoid ratios. *Proceedings from Ocean Optics XV*, October 16-20, Monaco.

Moore, C., M.S. **Twardowski**, and J.R.V. Zaneveld. 2000. The ECO VSF - A multi-angle scattering sensor for determination of the volume scattering function in the backward direction. *Proceedings from Ocean Optics XV*, October 16-20, Monaco.

**Twardowski**, M.S., E. Boss, J.B. Macdonald, W.S. Pegau, A.H. Barnard, and J.R.V. Zaneveld. 2000. A model for retrieving oceanic particle composition and size distribution from measurements of the backscattering ratio and spectral attenuation. *Proceedings from Ocean Optics XV*, October 16-20, Monaco.

**Twardowski**, M.S. 2000. Ocean research in the ocean state. *The Rhode Island State Trooper*, 12(1):107-109.

Boss, E., W.S. Pegau, W.D. Gardner, J.R.V. Zaneveld, A.H. Barnard, M.S. **Twardowski**, G.C. Chang, and T.D. Dickey. 2001. Spectral particulate attenuation in the bottom boundary layer of a continental shelf. *J. Geophys. Res.*, 106(C5):9509-9516. [refereed]

Boss, E., M.S. **Twardowski**, and S. Herring. 2001. Shape of the particulate beam attenuation spectrum and its inversion to obtain the shape of the particulate size distribution. *Appl. Opt.*, 40:4885-4893. [refereed]

Dekshenieks, M.M., P.L. Donaghay, J.M. Sullivan, J.E.B. Rines, T.R. Osborn, and M.S. **Twardowski**. 2001. Temporal and spatial occurrence of thin phytoplankton layers in relation to physical processes. *Mar. Ecol. Prog. Ser.*, **223**:61-71. [refereed]

**Twardowski**, M.S. and A. Barnard. 2001. Observing the ocean: sensing technology and observation platforms. *Maritimes*, 43(4).

**Twardowski**, M.S., and P.L. Donaghay. 2001. Separating in situ and terrigenous sources of absorption by dissolved material in coastal waters. *J. Geophys. Res.*, 106(C2):2545-2560. [refereed]

**Twardowski**, M.S., E. Boss, J.B. Macdonald, W.S. Pegau, A.H. Barnard, and J.R.V. Zaneveld. 2001. A model for estimating bulk refractive index from the optical backscattering ratio and the implications for understanding particle composition in Case I and Case II waters. *J. Geophys. Res.*, 106(C7):14,129-14,142. [refereed]

Gould, R., R. Stavn, M. **Twardowski**, and G. Lamella. 2002. Partitioning optical properties into organic and inorganic components from ocean color imagery. *Proceedings from Ocean Optics XVI*, November 18-22, Santa Fe, NM.

Rines, J.E.B., P.L. Donaghay, M. Dekshenieks, J.M. Sullivan, and M.S. **Twardowski**. 2002. Thin layers and camouflage: hidden *Pseudo-nitzschia spp*. (Bacillariophyceae) populations in a fjord in the San Juan Islands, Washington, U.S.A. *Mar. Ecol. Prog. Ser.*, 225:123-137. [refereed]

Sullivan, J.M., M.S. **Twardowski**, P.L. Donaghay, and S. Freeman. 2002. Particulate bulk refractive index distributions in coastal regions as determined from backscattering ratio measurements. *Proceedings from Ocean Optics XVI*, November 18-22, Santa Fe, NM.

**Twardowski**, M.S., and P.L. Donaghay. 2002. Photobleaching of aquatic dissolved materials: absorption removal, spectral alteration, and their interrelationship. *J. Geophys. Res*, 107(C8). [refereed]

**Twardowski**, M.S., J.R.V. Zaneveld, and C. Moore. 2002. A novel technique for determining beam attenuation compatible with a small sensor form factor and compact deployment platforms. *Proceedings from Ocean Optics XVI*, November 18-22, Santa Fe, NM.

Zaneveld, J.R.V., M.S**. Twardowski**, K.S. Shifrin, W.S. Pegau, E. Boss, and I. Zolotov. 2002. Inversion of light scattering measurements to obtain biogeochemical parameters. *Proceedings from Ocean Optics XVI*, November 18-22, Santa Fe, NM.

Dekshenieks, M.M., AL Alldredge, A Barnard, E Boss, J Case, TJ Cowles, PL Donaghay, LB Eisner, DJ Gifford, CF Greenlaw, C Herren, DV Holliday, D Johnson, S MacIntyre, D McGehee, TR Osborn, MJ Perry, R Pieper, JEB Rines, DC Smith, JM Sullivan, MK Talbot, MS **Twardowski**, A Weidemann and JR Zaneveld. 2003. Characteristics, Distribution and Persistence of Thin Layers Over a 48 Hour Period. *Mar. Ecol. Prog. Ser.*, 261:1-19. [refereed]

Eisner, L., M.S. **Twardowski**, and T.J. Cowles. 2003. Relationship between phytoplankton pigment composition and in situ spectral absorption measurements in East Sound, Orcas, Island, WA. *Limnol. Oceanogr.*, 48:632-646. [refereed]

Miller, R., M.S. **Twardowski**, C. Moore, and C. Casagrande. 2003. The Dolphin: Technology to Support Remote Sensing Bio-optical Algorithm Development and Applications. *Backscatter* 14(2):8-12. [refereed]

Boss, E., W. S. Pegau, M. Lee, M. S**. Twardowski**, E. Shybanov, G. Korotaev, and F. Baratange. 2004. The particulate backscattering ratio at LEO 15 and its use to study particles composition and distribution*. J. Geophys. Res.*, 109, C01014, doi:10.1029/2002JC001514. [refereed]

Moore, C., J. Da Cuhna, B. Rhoades, M.S. Twardowski, J.R.V. Zaneveld, J. Dombroski. 2004. A new in-situ measurement and analysis system for excitation-emission fluorescence in natural waters. *Proceedings of Ocean Optics XVII*, October 25-29, Freemantle, Australia.

Schofield, O., J. Kohut, J. Kerfoot, L. Creed, C. Mugdal, S. Glenn, M. **Twardowski**, C. Jones, and D. Webb. 2004. Dawn in the age of ocean robots: what can they see? *Proceedings of Ocean Optics XVII*, October 25-29, Freemantle, Australia.

Sullivan, J.M., M.S. **Twardowski**, J.R.V. Zaneveld, C. Moore, B. Rhoades, and R. Miller. 2004. The hyperspectral temperature and salinity dependent absorption coefficients of pure water. *Proceedings of Ocean Optics XVII*, October 25-29, Freemantle, Australia.

**Twardowski**, M.S., and J.R.V. Zaneveld. 2004. Progress toward a Generalized Optical-Biogeochemical Inversion (GOBI) for natural waters. *Proceedings of Ocean Optics XVII*, October 25-29, Freemantle, Australia.

**Twardowski**, M.S., E. Boss, J.M. Sullivan, and P.L. Donaghay. 2004. Modeling spectral absorption by chromophoric dissolved organic matter (CDOM**).** *Mar. Chem.*, 89: 69-88, doi:10.1016/j.marchem.2004.02.008. [refereed]

Zaneveld, J.R.V., C. Moore, A.H. Barnard, M.S. **Twardowski**, and G.C. Chang. 2004. Correction and analysis of spectral absorption data taken with the WET Labs AC-S. *Proceedings of Ocean Optics XVII*, October 25-29, Freemantle, Australia.

Sullivan, J.M., M.S. **Twardowski**, Donaghay, P.L., and Freeman, S.A. 2005. Using Scattering Characteristics to Discriminate Particle Types in US Coastal Waters, *Appl. Opt*., 44:1667-1680. [refereed]

Trees, C.C., P.W. Bissett, H,. Dierssen, D.D.R. Kohler, M.A. Moline, J.L. Mueller, R.E. Pieper, M.S. **Twardowski**, and J.R.V. Zaneveld. 2005. Monitoring water transparency and diver visibility in ports and harbors using aircraft hyperspectral remote sensing. *Prodeedings from SPIE Port and Harbor Security Conference,* Vol. 5780, February, Orlando, FL.

**Twardowski**, M.S., M. Lewis, A. Barnard, J.R.V. Zaneveld. 2005. In-water instrumentation and platforms for ocean color remote sensing applications. *In:* Remote Sensing of Coastal Aquatic Waters, R. Miller and C. Del-Castillo [Eds.], Springer-Kluwer Publishing, pp. 69-100. [refereed]

**Twardowski**, M.S., J.R.V. Zaneveld, C.M. Moore, J. Mueller, C. Trees, O. Schofield, S. Freeman, T. Helble, and G. Hong. 2005. Diver visibility measured with a compact scattering-attenuation meter (SAM) compatible with AUVs and other small deployment platforms. *Prodeedings from SPIE Port and Harbor Security Conference*, Vol. 5780, February, Orlando, FL.

Zaneveld, J.R.V., M.S. **Twardowski**, M. Lewis, and A. Barnard. 2005. Radiative transfer and remote sensing. *In*: Remote Sensing of Coastal Aquatic Waters, R. Miller and C. Del-Castillo [Eds.], Springer-Kluwer Publishing, pp. 1-20. [refereed]

Aurin, D., H. Dierssen, and M. **Twardowski**. 2006. Absorption, Backscatter and Chlorophyll Algorithms for Ocean Color Remote Sensing in Long Island Sound. *Proceedings of Ocean Optics XVIII*, October 9-13, Montreal, Canada.

Sullivan, J.M., M.S. **Twardowski**, J.R.V. Zaneveld, C. Moore, A. Barnard, P. Donaghay, and B. Rhoades. 2006. The hyperspectral temperature and salinity dependencies of absorption by water and heavy water in the 400-750 nm spectral range. *Appl. Opt.*, 45:5294-5309. [refereed]

**Twardowski** M., and M. Jonasz. 2006. VSF at the small angles for natural dispersions and power-law slopes (www.tpdsci.com/Tpc/VsfSmlAngNatDspSlp.php). In: *Topics in Particles and Dispersion Science* (www.tpdsci.com). [refereed]

**Twardowski** M., and M. Jonasz. 2006. Power law in spectral scattering by natural dispersions: Derivation (www.tpdsci.com/Tpc/AtnCfSptPwLwNatDsp.php). In: *Topics in Particles and Dispersion Science* (www.tpdsci.com). [refereed]

**Twardowski** M., and M. Jonasz. 2006. Power law in spectral scattering by natural dispersions: Finite range of the particle diameter (www.tpdsci.com/Tpc/AtnCfSptPwLwNatDsp.php). In: *Topics in Particles and Dispersion Science* (www.tpdsci.com). [refereed]

Zaneveld, J.R.V, M.S. **Twardowski**, and C. Moore. 2006. Total scattering coefficient meter. *Proceedings of Ocean Optics XVIII*, October 9-13, Montreal, Canada.

Huot, Y., M. Babin, F. Bruyant, C. Grob, M. S. **Twardowski**, and H. Claustre. 2007. Does chlorophyll *a* provide the best index of phytoplankton biomass for primary productivity studies? *Biogeosciences*, 4:853-868, www.biogeosciences.net/4/853/2007/. [refereed]

Huot, Y., A. Morel, M. **Twardowski**, D. Stramski, and R. Reynolds. 2007. Particle optical backscattering along a chlorophyll gradient in the upper layer of the eastern South Pacific. *Biogeosciences*, http://www.biogeosciences-discuss.net/4/4571/2007/bgd-4-4571-2007.pdf. [refereed]

Stramski, D., R. Reynolds, M. Babin, H. Claustre, S. Kaczmarek, M. Lewis, R. Rottgers, A. Sciandra, M. Stramska, and M. **Twardowski**. 2007. Relationships POC and optical properties of surface waters in the South Pacific and Atlantic Oceans. *Biogeosciences*, 5, 171-183. [refereed]

**Twardowski**, M.S., H. Claustre, S.A. Freeman, D. Stramski, and Y. Huot. 2007. Optical backscattering properties of the "clearest" natural waters. *Biogeosciences,* 4, 1041–1058, www.biogeosciences.net/4/1041/2007/. [refereed]

Bell, J., M. **Twardowski**, C. Moore, and A. Barnard. 2008. Comprehensive optical merge processing and acquisition software system (COMPASS) for comprehensive user correction of WET Labs absorption and attenuation data. *Proceedings of Ocean Optics XIX*, October 6-9, Barga, Italy.

Glenn, S., C. Jones, M. **Twardowski**, L. Bowers, J. Kerfoot, J. Kohut, D. Webb, and O. Schofield. 2008. Glider observations of sediment resuspension in a Middle Atlantic Bight fall transition storm. *Limnol. Oceanogr.,* 53(5, part II), 2180-2196.

Moore, C., J. Koegler, W. Strubhar, M. **Twardowski**, A. Barnard, A. Derr, and R. Zaneveld. 2008. The next generation beam attenuation meter (BAM) for autonomous underwater vehicles. *Proceedings of Ocean Optics XIX*, October 6-9, Barga, Italy.

Nencioli, F., G. Chang-Spada, and M. **Twardowski**. 2008. Optical Characterization of an Eddy Induced Diatom Bloom West of the Island of Hawaii. *Proceedings of Ocean Optics XIX*, October 6-9, Barga, Italy.

Sciandre, A., D. Stramski, M. Babin, M. **Twardowski**, and C. Grob. 2008. Diel and spatial variability of particle size distribution in the eastern south Pacific. *Proceedings of Ocean Optics XIX*, October 6-9, Barga, Italy.

Tonizzo, A., J. Zhou, A. Gilerson, T. Iijima, M. **Twardowski**, D. Gray, R. Arnone, B. Gross, F. Moshary, and S. Ahmed .2008. Polarization measurements in coastal waters using hyperspectral multi-angular sensor. *Proceedings of Ocean Optics XIX*, October 6-9, Barga, Italy.

**Twardowski**, M., S. Freeman, X. Zhang, S. Vagle, and R. Zaneveld. 2008. Resolving surf zone particle dynamics with high sampling rate volume scattering function measurements. *Proceedings of Ocean Optics XIX*, October 6-9, Barga, Italy.

Zhang, X., M. **Twardowski**, C. Hu, and M. Lewis. 2008. Retrieving size and optical properties of individual particle populations from the volume scattering function. *Proceedings of Ocean Optics XIX*, October 6-9, Barga, Italy.

Aurin, D., H.M. Dierssen, M.S. **Twardowski**, and C.S. Roesler. 2009. Optical complexity in Long Island Sound and implications for coastal ocean color remote sensing. *Journal of Geophysical Research*, in press.

Gordon, H.R., M.R. Lewis, S.D. McLean, M.S. **Twardowski**, S.A. Freeman, K.J. Voss, and G.C. Boynton. 2009. Spectra of particulate backscattering in natural waters. *Optics Express*, 17(18), 16192-16208.

Nencioli, F., G. Chang, M. **Twardowski**, and T.D. Dickey. 2009. Optical Characterization of an eddy-induced diatom bloom west of the island of Hawaii. *Biogeosciences*, in press.

Sullivan, J.M., and M.S. **Twardowski**. 2009. Angular shape of the volume scattering function in the backward direction. *Applied Optics*, in press.

Tonizzo, A., J. Zhou, A. Gilerson, M. **Twardowski**, D. Gray, R. Arnone, B. Gross, F. Moshary, and S. Ahmed. 2009. Polarization measurements in coastal waters: hyperspectral and multiangular analysis. *Optics Express*, **17**, 5666-5683.

Voss, K.J., S. McLean, M. Lewis, C. Johnson, S. Flora, M. Feinholz, M. Yarbrough, C. Trees, M. **Twardowski**, and D. Clark. 2009. An example crossover experiment for testing new vicarious calibration techniques for satellite ocean color radiometry. *Journal of Atmospheric and Oceanic Technology*, in press.

Zhang, X., L. Hu, M.S. **Twardowski**, and J.M. Sullivan. 2009. Scattering by solutions of major sea salts. *Optics Express*, in press.

**PATENTS**

None.

**HONORS/AWARDS/PRIZES**

Twardowski, M., 2005: *Spinoff* technology selection, NASA Innovative Partnership Program, http://www.sti.nasa.gov/tto/Spinoff2005/PDF/accessible.pdf, p. 62.

Twardowski, M., 2003: Adjunct Professor, University of Rhode Island.

Twardowski, M., 2000: ASEE Visiting Faculty Fellowship, Naval Research Labs.

Twardowski, M., 2000: Early Career Faculty Award, Office of International Research and Development, Oregon State University.

Twardowski, M., 1998: WET Labs Environmental Optics Postdoctoral Fellowship, Oregon State University.